

Electroconductive Porous Coordination Polymer Cu[Cu(pdt)₂] Composed of Donor and Acceptor Building Units

Shinya Takaishi,^{*,†} Miyuki Hosoda,[†] Takashi Kajiwara,[†] Hitoshi Miyasaka,[†] Masahiro Yamashita,[†] Yasuyuki Nakanishi,[‡] Yasutaka Kitagawa,[‡] Kizashi Yamaguchi,[§] Atsushi Kobayashi,^{||,⊥} and Hiroshi Kitagawa^{||,♯}

[†]Department of Chemistry, Graduate School of Science, Tohoku University, 6-3 Aza-Aoba, Aramaki, Aoba-ku, Sendai 980-8575, Japan, [‡]Department of Chemistry, Graduate School of Science, Osaka University, 1-1 Machikaneyama-cho, Toyonaka, Osaka 560-0043, Japan, [§]Center for Quantum Science and Technology under Extreme Conditions, Osaka University, 1-3 Machikaneyama-cho, Toyonaka, Osaka 560-8531, Japan, ^{||}Graduate School of Science, Kyushu University, 6-10-1 Hakozaki, Higashi, Fukuoka 812-8581, Japan, and [♯]CREST (JST), 4-1-8 Hon-cho, Kawaguchi-shi, Saitama 332-0012, Japan. [⊥]Present address: Hokkaido University, Kita 10, Nishi 8, Kita-ku, Japan

Received November 5, 2008

We synthesized a new porous coordination polymer Cu[Cu(pdt)₂], which shows relatively high electrical conductivity ($6 \times 10^{-4} \text{ S cm}^{-1}$ at 300 K) by the introduction of electron donors and acceptors as building units. This compound is applicable as a porous electrode with high power density. In addition, this compound forms a triangular spin lattice and shows spin frustration.

Porous coordination polymers (PCPs) or metal–organic frameworks have attracted considerable interest as a new class of micro- or mesoporous materials with huge surface area, regularity, and flexibility. These compounds have been extensively studied in the past decade because of their potential application for the fuel storage,¹ separation,² catalysis,³ etc. Recently, there has been growing interest in the physical

properties of PCPs such as magnetic⁴ and photoluminescence⁵ responses. However, almost no attention has been paid to their electrical conductivity. To the best of my knowledge, there is only one PCP that shows relatively high electrical conductivity.⁶ If a PCP with high electric conductivity is realized, it is applicable to a porous electrode for batteries, fuel cells, capacitors, etc. Because PCPs have potentially huge surface areas, these compounds have a good potential as such electrodes with high power density. Here we report the synthesis, crystal structure, and physical properties of a novel electroconductive PCP, Cu[Cu(pdt)₂] (pdt = 2,3-pyrazinedithiolate). In order to acquire the electroconductive property, we used electron donors and acceptors as building units.

Figure 1 shows the molecular structure of the electron acceptor unit [Cu^{III}(pdt)₂][−], which was reported by Rovira et al.⁷ They have shown that this molecule shows a reversible redox process between [Cu^I(pdt)₂]^{2−} and [Cu^{III}(pdt)₂][−] at $-0.33 \text{ V vs Ag/AgCl}$, indicating that [Cu^{III}(pdt)₂][−] can act as an electron acceptor. In addition, this molecule has four coordination sites (N atoms of the pyrazine moiety). Therefore, this molecule can be used as the redox-active linker unit of the PCP. We chose the Cu^I ion as a connector unit. It has been known that the Cu^I ion acts as an electron donor,⁸ stable

*To whom correspondence should be addressed. E-mail: takaishi@agnus.chem.tohoku.ac.jp.

(1) (a) Rowsell, J. L. C.; Yaghi, O. M. *Angew. Chem., Int. Ed.* **2005**, *44*, 4670–4679. (b) Matsuda, R.; Kitaura, R.; Kitagawa, S.; Kubota, Y.; Belosludov, R. V.; Kobayashi, T. C.; Sakamoto, H.; Chiba, T.; Takata, M.; Kawazoe, Y.; Mita, Y. *Nature* **2005**, *436*, 238–241. (c) Chen, B.; Fronczek, F. R.; Maverick, A. W. *Inorg. Chem.* **2004**, *43*, 8209–8211.

(2) (a) Tanaka, D.; Nakagawa, K.; Higuchi, M.; Horike, S.; Kubota, Y.; Kobayashi, T. C.; Takata, M.; Kitagawa, S. *Angew. Chem., Int. Ed.* **2008**, *47*, 3914–3918. (b) Ma, S.; Wang, X.-S.; Yuan, D.; Zhou, H.-C. *Angew. Chem., Int. Ed.* **2008**, *47*, 4130–4133. (c) Maji, T. K.; Uemura, K.; Chang, H.-C.; Matsuda, R.; Kitagawa, S. *Angew. Chem., Int. Ed.* **2004**, *43*, 3269–3272.

(3) (a) Maggard, P. A.; Yan, B. B.; Luo, J. H. *Angew. Chem., Int. Ed.* **2005**, *44*, 2553–2556. (b) Wu, C. D.; Hu, A.; Zhang, L.; Lin, W. *J. Am. Chem. Soc.* **2005**, *127*, 8940–8941. (c) Kitaura, R.; Onoyama, G.; Sakamoto, H.; Matsuda, R.; Noro, S.; Kitagawa, S. *Angew. Chem., Int. Ed.* **2004**, *43*, 2684–2687. (d) Seo, J. S.; Whang, D.-M.; Lee, H.-Y.; Jun, S. I.; Oh, J.-H.; Jeon, Y.-J.; Kim, K.-M. *Nature* **2000**, *404*, 982–986. (e) Sawaki, T.; Aoyama, Y. *J. Am. Chem. Soc.* **1999**, *121*, 4793–4798.

(4) (a) Yanai, N.; Kaneko, W.; Yoneda, K.; Ohba, M.; Kitagawa, S. *J. Am. Chem. Soc.* **2007**, *129*, 3496–3497. (b) Ohba, M.; Kaneko, W.; Kitagawa, S.; Maeda, T.; Mito, M. *J. Am. Chem. Soc.* **2008**, *130*, 4475–4484. (c) Halder, G. J.; Kepert, C. J.; Moubaraki, B.; Murray, K. S.; Cashion, J. D. *Science* **2002**, *298*, 1762–1765. (d) Maspoeh, D.; Ruiz-Molina, D.; Wurst, K.; Domingo, N.; Cavallini, M.; Biscarini, F.; Tejada, J.; Rovira, C.; Veciana, J. *Nat. Mater.* **2003**, *2*, 190–195.

(5) Kato, M.; Omura, A.; Toshikawa, A.; Kishi, S.; Sugimoto, Y. *Angew. Chem., Int. Ed.* **2002**, *41*, 3183–3185.

(6) Fuma, Y.; Ebihara, M.; Kutsumizu, S.; Kawamura, T. *J. Am. Chem. Soc.* **2004**, *126*, 12238–12239.

(7) Ribas, X.; Dias, J. C.; Morgado, J.; Wurst, K.; Molins, E.; Ruiz, E.; Almeida, M.; Veciana, J.; Rovira, C. *Chem.—Eur. J.* **2004**, *10*, 1691–1704.

(8) (a) Hüning, S. *J. Mater. Chem.* **1995**, *5*, 1469–1479. (b) Aumüller, A.; Erk, P.; Klebe, G.; Hüning, S.; von Schuts, J. U.; Werner, H.-P. *Angew. Chem., Int. Ed.* **1986**, *25*, 740–741. (c) Kato, R. *Bull. Chem. Soc. Jpn.* **2000**, *73*, 515–534. (d) Kawamoto, A.; Miyagawa, K.; Kanoda, K. *Phys. Rev. Lett.* **2001**, *87*, 107602. (e) Kobayashi, H.; Miyamoto, A.; Kato, R.; Sakai, F.; Kobayashi, A.; Yamakita, Y.; Furukawa, Y.; Tatsumi, M.; Watanabe, T. *Phys. Rev. B.* **1993**, *47*, 3500–3510. (f) Tadokoro, M.; Yasuzuka, S.; Nakamura, M.; Shinoda, T.; Toshinori, T.; Mitsumi, M.; Ozawa, Y.; Toriumi, K.; Yoshino, H.; Shimoi, D.; Sato, K.; Takui, T.; Mori, T.; Murata, K. *Angew. Chem., Int. Ed.* **2006**, *45*, 5144–5147.

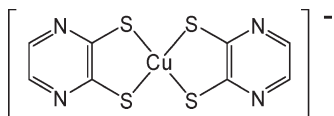


Figure 1. Molecular structure of $[\text{Cu}^{\text{III}}(\text{pdt})_2]^-$.

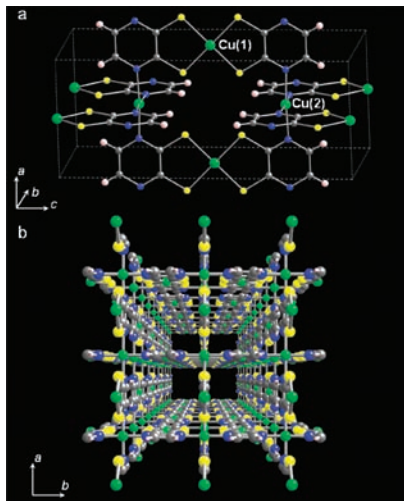


Figure 2. (a) Crystal structure in $\text{Cu}[\text{Cu}(\text{pdt})_2]$. (b) Perspective view of the crystal structure of $\text{Cu}[\text{Cu}(\text{pdt})_2]$. Color code: green, Cu; yellow, S; gray, C; blue, N; pink, H.

with a coordination number of 4 or 6 with different ligands. According to such a strategy, we have synthesized the novel PCP $\text{Cu}[\text{Cu}(\text{pdt})_2]$.

Single crystals of $\text{Cu}[\text{Cu}(\text{pdt})_2]$ were synthesized by the slow diffusion of CuI and $\text{Na}[\text{Cu}(\text{pdt})_2] \cdot 2\text{H}_2\text{O}$ in an acetonitrile solution in an H-shaped cell. The crystal structure was determined in a single crystal by the Bruker SMART CCD diffractometer with graphite-monochromated $\text{Mo K}\alpha$ radiation ($\lambda = 0.7107 \text{ \AA}$). Magnetic susceptibility was acquired with a Quantum design MPMS-XL SQUID magnetometer. Electrical conductivity measurements were carried out using a Agilent 34420A nanovoltmeter. IR spectroscopy measurement was carried out with a KBr pellet using a Thermo Nicolet NEXUS 670 FT/IR spectrometer.

Figure 2 shows the crystal structure of $\text{Cu}[\text{Cu}(\text{pdt})_2]$. In this compound, N atoms of the pyrazine moiety coordinate to Cu ions, forming an infinite tetragonal lattice, as shown in Figure 2b. One-dimensional vacant spaces of $3.4 \text{ \AA} \times 3.4 \text{ \AA}$ exist within the framework. Considering charge neutrality, there are two possibilities of electronic states of the compound, which are $\text{Cu}^{\text{II}}[\text{Cu}^{\text{II}}(\text{pdt})_2]$ and $\text{Cu}^{\text{I}}[\text{Cu}^{\text{III}}(\text{pdt})_2]$. We assumed that this compound is in the $\text{Cu}^{\text{II}}[\text{Cu}^{\text{II}}(\text{pdt})_2]$ state through analysis of the $\text{Cu}(1)\text{--S}$ distance. The $\text{Cu}(1)\text{--S}$ distance of the present compound is 2.264 \AA , which is longer than that of $\text{Na}[\text{Cu}^{\text{III}}(\text{pdt})_2] \cdot 2\text{H}_2\text{O}$ (2.181 and 2.183 \AA). As Rovira et al. have indicated, the lowest unoccupied molecular orbital of $[\text{Cu}^{\text{III}}(\text{pdt})_2]^-$ is formed by an antibonding orbital of Cu $d_{x^2-y^2}$ and S p_σ .⁷ Therefore, the $\text{Cu}(1)\text{--S}$ distance should become longer when $[\text{Cu}^{\text{III}}(\text{pdt})_2]^-$ is reduced to $[\text{Cu}^{\text{II}}(\text{pdt})_2]^{2-}$. Meanwhile, the valency of $\text{Cu}(2)$ can be estimated to be Cu^{II} because the $\text{Cu}\text{--N}_4$ geometry is slightly distorted square planar (distortion angle = 6.45°) rather than tetrahedral. In the X-ray crystal structure analysis, although some residual electron densities were observed within the micropore, these were probably due to the solvent molecules, but assignment to a specific molecule cannot be made (see the Supporting Information).

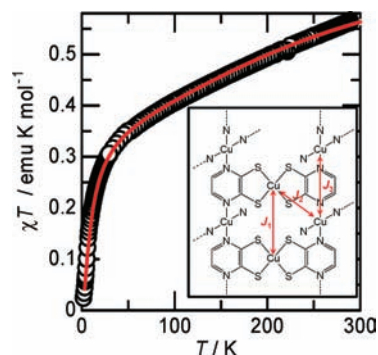


Figure 3. Temperature dependence of magnetic susceptibility in $\text{Cu}[\text{Cu}(\text{pdt})_2]$. Inset: three possible pathways of magnetic interactions: J_1 , $\text{Cu}(1)\text{--S}\cdots\text{S}\text{--Cu}(1)$; J_2 , $\text{Cu}(1)\text{--S}\text{--C}\text{--N}\text{--Cu}(2)$; J_3 , $\text{Cu}(2)\text{--N}\text{--C}\text{--C}\text{--N}\text{--Cu}(2)$. The red line shows the best fit to the summation of eqs 1 and 2.

Figure 3 shows the temperature dependence of magnetic susceptibility in $\text{Cu}[\text{Cu}(\text{pdt})_2]$. Because magnetic susceptibility showed paramagnetic behavior in the entire temperature range, we were convinced that this compound was in the divalent $\text{Cu}^{\text{II}}[\text{Cu}^{\text{II}}(\text{pdt})_2]$ state. Rovira et al. have synthesized the coordination polymer $\text{Cu}[\text{Cu}(\text{pds})_2]$ ($\text{pds} = 2,3\text{-pyrazine-diselenol}$) with a two-dimensional layered structure by electrolysis of $\text{Na}[\text{Cu}(\text{pds})_2] \cdot 2\text{H}_2\text{O}$,⁹ which is in the diamagnetic $\text{Cu}^{\text{I}}[\text{Cu}^{\text{III}}(\text{pds})_2]$ state. We have also obtained the same crystal by the slow diffusion of $\text{Na}[\text{Cu}(\text{pds})_2] \cdot 2\text{H}_2\text{O}$ and CuI in an acetonitrile solution. This difference of the electronic state is probably due to the lower redox potential of $[\text{Cu}^{\text{III}}(\text{pds})_2]^-$ (-0.54 V vs Ag/AgCl) than $[\text{Cu}^{\text{III}}(\text{pdt})_2]^-$ (-0.33 V vs Ag/AgCl).⁷

Here we consider the possible pathways of magnetic interaction. As shown in the inset of Figure 3, three magnetic interactions are possible in the crystal. In order to estimate those magnetic couplings by theoretical calculations, we constructed three model structures consisting of two Cu^{II} ions, as illustrated in Figure S1 in the Supporting Information. Models A–C represent the magnetic interactions J_1 , J_2 , and J_3 . For these models, the unrestricted B3LYP¹⁰ (UB3LYP) method was carried out on Gaussian98.¹¹ All calculations were performed by use of the MIDI + p basis set¹² for Cu atoms and the 4-31G basis set for others. Because the Cu^{II} ion has one spin, singlet and triplet spin couplings are expected in the models. Therefore, the J value in the Heisenberg Hamiltonian $\hat{H} = -2J\hat{S}_i \cdot \hat{S}_j$ can be calculated by the energy gap between the singlet and triplet states.¹³ Calculated total energies and $\langle S^2 \rangle$ values are summarized in Table S1 in the Supporting

(9) Ribas, X.; Maspoch, D.; Dias, J.; Morgado, J.; Almeida, M.; Wurst, K.; Vaughan, G.; Veciana, J.; Rovira, C. *CrystEngComm* **2004**, *6*, 589–592.

(10) Becke, A. D. *J. Chem. Phys.* **1993**, *98*, 5648–5652.

(11) Frisch, M. J.; et al. *Gaussian 98*, revision A.11.3; Gaussian, Inc.: Pittsburg, PA, **2002**.

(12) Gaussian basis sets for molecular calculations: Huzinaga, S., Ed. *Physical Sciences Data 16*; Elsevier: New York, **1984**.

(13) J values are calculated by the Yamaguchi equation,

$$J = \frac{E^{\text{singlet}} - E^{\text{triplet}}}{\langle S^2 \rangle^{\text{singlet}} - \langle S^2 \rangle^{\text{triplet}}} \quad (3)$$

where E and $\langle S^2 \rangle$ denote the total energy and the total spin angular momentum, respectively. This equation is explained in: Kawakami, T.; Yamanaka, S.; Yamada, S.; Mori, W.; Yamaguchi, K. In *Molecular-Based Magnetic Materials, Theory, Technique and Applications*; Turnbull, M. M., Sugimoto, T., Thompson, L. K., Eds.; ACS Symposium Series 644; American Chemical Society: Washington, DC, **1996**; p 30.

Information. The estimated magnitudes of the magnetic interactions are $J_1/k_B = -353.2$ K, $J_2/k_B = 25.1$ K, and $J_3/k_B = -13.6$ K. Although quantitatively may not be enough because this calculation was performed with two distinct units, we can assume that the relationship between the three values is $J_1 \gg J_2, J_3$. In addition, considering the geometry of the magnetic interaction, there can be magnetic frustrations, e.g., $-J_1-J_2-J_2-$ and $-J_2-J_3-J_3-$, because they form triangular lattices. Because J_1 is much larger than J_2 , we can ignore the contribution of J_2 . In this situation, the contribution of J_3 is independent of that of J_1 . Therefore, we fitted the measured magnetic susceptibility by the summation of a one-dimensional Heisenberg antiferromagnetic model (Bonner–Fisher model)¹⁴ for J_1 and a two-dimensional Heisenberg antiferromagnetic model¹⁵ for J_3 as shown eqs 1 and 2.

$$\chi_{1D} = \frac{Ng^2\mu_B^2}{k_B T} \left(\frac{0.25 + 0.14995x_1 + 0.30094x_1^2}{1 + 1.9862x_1 + 0.68854x_1^2 + 6.0626x_1^3} \right) \quad (1)$$

where $x_1 = J_1/k_B T$

$$\chi_{2D} = \frac{Ng^2\mu_B^2}{k_B T} \times \left(\frac{0.25}{1 + 2x_3 + 2x_3^2 + 1.333x_3^3 + 0.250x_3^4 - 0.4833x_3^5 + 0.003797x_3^6} \right) \quad (2)$$

where $x_3 = J_3/k_B T$.

The parameters obtained are $J_1/k_B = -162.6$ K, $J_3/k_B = -4.1$ K, and $g = 2.007$. Hendrickson et al. reported the pyrazine-bridged two-dimensional compound $\text{Cu}^{\text{II}}(\text{pyz})_2(\text{ClO}_4)_2$ and showed that this compound has weak antiferromagnetic interaction ($J = -7.6$ K), which is consistent with our result.¹⁶

Figure 4 shows the temperature dependence of the electrical conductivity in $\text{Cu}[\text{Cu}(\text{pdt})_2]$. This compound showed relatively high electrical conductivity ($6 \times 10^{-4} \text{ S cm}^{-1}$ at 300 K). The temperature dependence of the electrical conductivity showed semiconductive behavior, and an activation energy was determined to be 193 meV from the Arrhenius fitting of the conductivity. The reason for such a relatively high electrical conductivity is probably the charge bistability between $\text{Cu}^{\text{I}}[\text{Cu}^{\text{III}}(\text{pdt})_2]$ and $\text{Cu}^{\text{II}}[\text{Cu}^{\text{II}}(\text{pdt})_2]$.

Figure 5 shows the IR spectrum of $\text{Cu}^{\text{II}}[\text{Cu}^{\text{II}}(\text{pdt})_2]$ at room temperature. A broad peak at approximately 0.7 eV was observed, but it was not observed in $\text{Na}[\text{Cu}(\text{pdt})_2]$. We

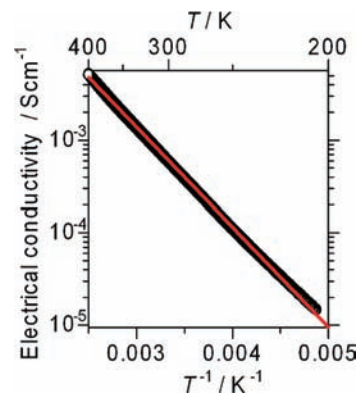


Figure 4. Temperature dependence of the electrical conductivity in $\text{Cu}[\text{Cu}(\text{pdt})_2]$. The red line shows the best fit to the Arrhenius model.

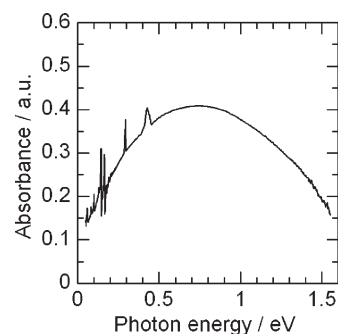


Figure 5. IR spectrum of $\text{Cu}[\text{Cu}(\text{pdt})_2]$.

assigned this peak as the charge-transfer (CT) band from $\text{Cu}^{\text{II}}[\text{Cu}^{\text{II}}(\text{pdt})_2]$ to $\text{Cu}^{\text{I}}[\text{Cu}^{\text{III}}(\text{pdt})_2]$ states because the peak energy is too low to assign to an intramolecular transition. Torrance et al. have reported that a series of CT complexes with alternately stacked structures have CT transitions in the IR region and some of them show phase transition accompanied by CT.¹⁷ In the present case, however, no anomaly was observed in the electrical conductivity and magnetic susceptibility, showing that the $\text{Cu}^{\text{II}}[\text{Cu}^{\text{II}}(\text{pdt})_2]$ state is stable in the measured temperature range (2–400 K). This is probably due to the large rearrangement energy between square-planar Cu^{II} and tetrahedral Cu^{I} geometries.

Acknowledgment. This work was partly supported by a Grant-in-Aid for Creative Scientific Research from the Ministry of Education, Culture, Sports, Science and Technology.

Supporting Information Available: Crystallographic data of $\text{Cu}[\text{Cu}(\text{pdt})_2]$ (CIF), model structures used for the theoretical calculations, calculated total energies, and refinement of the electron density within the pore. This material is available free of charge via the Internet at <http://pubs.acs.org>.

(14) (a) Bonner, J. C.; Fisher, M. E. *Phys. Rev.* **1964**, *135*, A640–A658. (b) Estes, W. E.; Gavel, D. P.; Hatfield, W. E.; Hodgson, D. J. *Inorg. Chem.* **1978**, *17*, 1415–1421.

(15) (a) Rushbrooke, G. S.; Wood, P. J. *Mol. Phys.* **1958**, *1*, 257–283. (b) Lines, M. E. *J. Phys. Chem. Solids* **1970**, *31*, 101–116.

(16) Darriet, J.; Haddad, M. S.; Duesler, E. N.; Hendrickson, D. N. *Inorg. Chem.* **1979**, *18*, 2679–2682.

(17) Torrance, J. B.; Vazquez, J. E.; Mayerle, J. J.; Lee, V. Y. *Phys. Rev. Lett.* **1981**, *46*, 253–257.